PHYSICAL REVIEW C **76**, 021304(R) (2007)

Shell evolution and the $N = 34$ "magic number"

M. Rejmund,[1] S. Bhattacharyya,[1,*] A. Navin,[1] W. Mittig,[1] L. Gaudefroy,[1,†] M. Gelin,[1] G. Mukherjee,[1,*] F. Rejmund,[1] P. Roussel-Chomaz,[1] and Ch. Theisen[2]

[1]*Grand Accélérateur National d'Ions Lourds (GANIL), CEA/DSM - CNRS/IN2P3, Bd Henri Becquerel, BP 55027, F-14076 Caen Cedex 5, France*

[2]*CEA-Saclay DSM/DAPNIA/SPhN, F-91191 Gif/Yvette Cedex, France*

(Received 27 November 2006; revised manuscript received 28 June 2007; published 28 August 2007)

Measurements of de-excitation γ rays in coincidence with target-like residues produced in deep inelastic transfer reactions of ^{238}U on a ^{48}Ca target at an energy near the Coulomb barrier are presented. A systematic analysis, within a shell model approach, of the measured low-lying states in the odd and even neutron-rich Ca isotopes points toward a possible absence of a predicted shell closure at $N = 34$.

DOI: 10.1103/PhysRevC.76.021304 PACS number(s): 21.60.Cs, 23.20.Lv, 25.70.Lm, 27.40.+z

Energy shells or periodic enhancements of level densities from their mean value, as a function of energy, are a general feature arising from quantum effects in finite size systems ranging from atoms and nuclei to metallic clusters. Advances in the measurements of the size of large metallic clusters provided opportunities for the search for the existence of "super shells" and for "magic" numbers different from those in atomic and nuclear physics [1]. The improved sensitivity of experimental techniques, both with low-intensity radioactive ion beams and high-intensity stable beams, played an analogous role in the quest for understanding the evolution of the ordering of single-particle (shell model) states or new "magic numbers," as a function of isospin in nuclei far from stability [2]. Intense theoretical efforts are underway to obtain new effective shell model interactions that can explain and predict features of nuclei far from stability [3–6].

With the addition of protons in the $\pi 1f_{7/2}$ orbital, moving from Ca to Ni, the strongly attractive proton-neutron spin-flip interaction [6] is known to modify the ordering of the levels in the fp shell from $2p_{3/2}$, $2p_{1/2}$, and $1f_{5/2}$ in ^{49}Ca to $2p_{3/2}$, $1f_{5/2}$, and $2p_{1/2}$ in ^{57}Ni [7]. A similar migration of single-particle levels for changing N/Z asymmetry gives rise to weakening of known shell closures at $N = 8$, 20, 28 and the appearance of new ones, such as $N = 14$, 16, 32. An experimental indication of a subshell closure at $N = 32$ (between the $2p_{3/2}$ and $2p_{1/2}$ orbitals) was first shown in ^{52}Ca [8] and ^{56}Cr [9] from measurements following β decay and in ^{54}Ti [10] combining results from β decay and prompt γ spectroscopy using deep inelastic transfer reactions. The existence of a gap at $N = 34$ was first predicted more than 30 years back [11]. A recent prediction [5] of the existence of a "magic number" at $N = 34$ initiated a large experimental effort in neutron-rich nuclei around Ca [12–15]. No evidence for the appearance of a new gap at $N = 34$ was reported in Ti and Cr isotopes [12–14]. These nuclei are easier to study due to their lower N/Z values, but the presence of valence protons outside the $Z = 20$ shell reduces their sensitivity to the neutron configuration (hence the $N = 34$ closure) as compared to the more exotic neutron-rich isotopes of Ca. The study of these neutron-rich Ca isotopes also provides a good handle to explore the role of the $T = 1$ term of the nucleon-nucleon interaction in the evolution of shell structure far from stability.

Calculations using the most recent shell model interactions, GXPF1A [5] and KB3G [3], and KB3G's modification KB3GM [16], derived for nuclei having their valence nucleons in the pf shell, are in good overall agreement with the measured level schemes [3,5]. The GXPF1A interaction is obtained from a systematic fit to experimental data starting from a realistic interaction, while KB3GM is obtained from empirical modifications of the monopole part of the realistic nucleon-nucleon interaction. Shell model calculations using the GXPF1A interaction predicted a new shell closure at $N = 34$, based on an increasing energy gap between the $p_{1/2}$ and $f_{5/2}$ orbitals, making $^{54}_{20}Ca_{34}$ a new doubly "magic" nucleus [5]. Contrary to the above, the use of the KB3G/KB3GM interaction does not predict the appearance of this shell closure [5,16]. It should be noted that both interactions predict the low-lying states in the Ca isotopes to be dominated by valence single neutron excitations.

The rapidly decreasing production cross sections associated with the increasing N/Z values for ^{53,54}Ca make them difficult to characterize. Both the lack of experimental observation of ^{54}Ca and the small probability to populate the $f_{5/2}$ state in ^{53}Ca through β decay [15] make the verification of the above prediction difficult. Therefore, in the present work, excited states corresponding to dominant neutron single-particle configurations in neutron-rich isotopes of Ca ($^{50-52}$Ca) have been populated and identified to infer the difference in energy between the $p_{1/2}$ and $f_{5/2}$ orbitals and thus the shell gap at $N = 34$.

Deep inelastic collisions (DIC) near the Coulomb barrier have been shown to be a powerful way to populate neutron-rich nuclei far from stability [17]. Measurements using DIC have been made recently to study neutron-rich nuclei in this mass region both at Gammasphere with thick targets [10,13,18] and at PRISMA-CLARA with thin targets in direct kinematics

*Present address: VECC, 1/AF Bidhan Nagar, Kolkata 700 064, India.

†Present address: CEA/DIF/DPTA/SPN, B.P. 12, F-91680 Bruyères-le-Châtel, France.

[14]. The present work reports results obtained from deep inelastic reactions in inverse kinematics using the VAMOS-EXOGAM setup.

The measurements were made at GANIL using typical beam currents of $\simeq$2 pnA of ^{238}U from the CSSI cyclotron, at an energy of 1.31 GeV incident on a 1 mg/cm^2 thick, enriched ^{48}Ca target. The resulting target-like residues, produced in deep inelastic transfer reactions [2], were detected and identified using the large acceptance spectrometer VAMOS [19]. The optical axis of the spectrometer was placed at 35° (a calculated grazing angle) with respect to the beam axis. The focal plane detection system consisted of two position sensitive drift chambers separated by a distance of 1 m, a secondary electron (timing) detector (SeD), placed between the two drift chambers, and a segmented ionization chamber followed by a 21-element Si wall. The measured positions and angles x, y, θ, and ϕ at the focal plane and the magnetic field combined with ion optics were utilized to reconstruct the magnetic rigidity ($B\rho$), the scattering angle, and the path length for each fragment, on an event by event basis. The mass (A) and mass over charge (A/Q), used to identify the charged state of the nuclei, were obtained from the time of flight (distance of $\sim$7.5 m) and total energy and the reconstructed $B\rho$, respectively. The unambiguous identification (Z, A) of the various target-like residues can be seen in Fig. 1, which shows a typical identification matrix of energy loss and mass over charge for one charge state, for a section of the focal plane. As can be seen from Fig. 1, ^{53}Ca is the most neutron-rich isotope of Ca produced in the present work ($N/Z = 1.65$). The coincident prompt γ rays from the target-like residues were detected using 11 segmented clover detectors of the EXOGAM [20] array (photopeak efficiency $\sim$9% at 1 MeV) surrounding the target. The angle between the segment of the clover detector and the reconstructed velocity from the VAMOS spectrometer was used to correct for the Doppler effect on an event by event basis. The resulting γ-ray spectra obtained in coincidence with neutron-rich Ca isotopes identified in VAMOS are shown in Fig. 2.

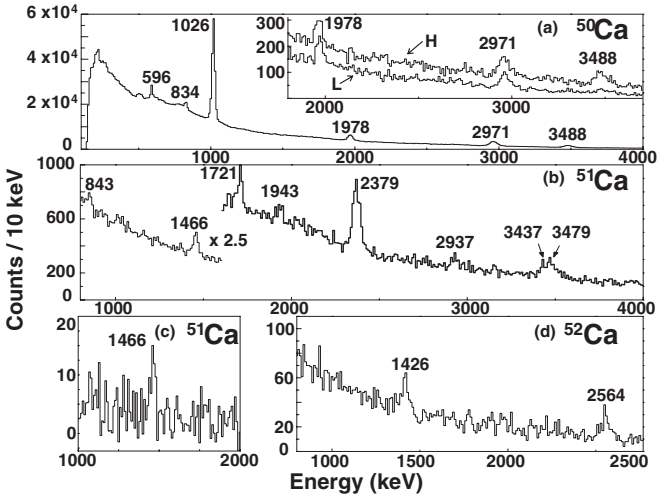

FIG. 2. Doppler corrected γ-ray spectra for different isotopes of calcium identified in the spectrometer. (a) ^{50}Ca, the inset shows the high energy part of the spectra for two different (L, low; H, high) excitation energy cuts; (b) ^{51}Ca; (c) portion of ^{51}Ca γ-ray spectra in coincidence with the 2379 keV transition; and (d) ^{52}Ca.

The level schemes for $^{50-52}$Ca obtained from the present work are shown in Fig. 3. These are based on measured γ-γ coincidences, relative intensities, and available data from Refs. [2,8,15,21] and were also guided by simple shell model arguments. The use of γ-γ coincidences was not possible in ^{52}Ca because of the limited statistics. The relative intensities of various transitions as a function of the excitation energy in the fragment were used as an additional aid for the placement of the γ rays. The excitation energy of the detected fragment was constrained from its measured kinetic energy. Such a method, to the best of our knowledge, has been employed for the first

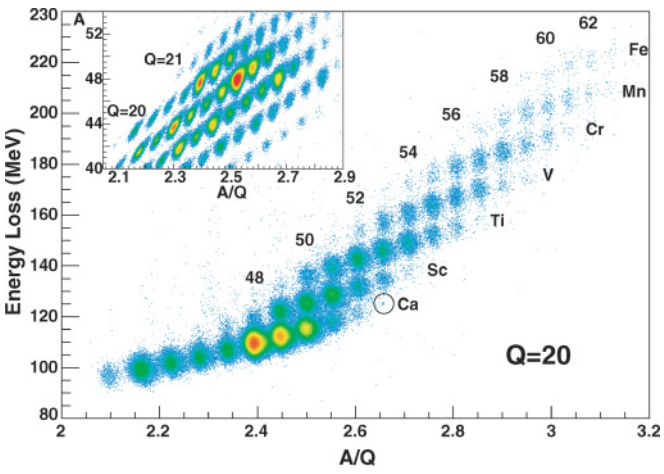

FIG. 1. (Color online) Energy loss versus the derived mass over charge (A/Q) for a selected charge state, $Q = 20$. The position of ^{53}Ca is indicated by the circle. The inset shows the corresponding mass (A) versus mass/charge (A/Q) used to identify the charged states. (See text.)

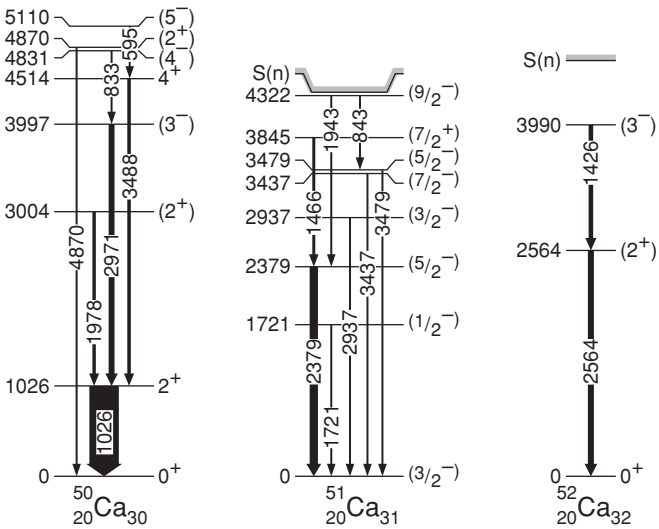

FIG. 3. Level schemes of the Ca isotopes as derived in the present measurement. The electromagnetic transitions are indicated by arrows; the widths indicate their relative intensities.

time. The inset in Fig. 2(a) shows a part of the γ spectra for two different (H, high; L, low) excitation energy cuts (normalized to the number of counts in the cut). The spectra corresponding to a higher excitation energy (H) show a relatively larger yield for the known higher lying 4^+ state, which decays by a 3488 keV γ ray, compared to that of the lower excitation energy (L). In ^{50}Ca the 1978.2(0.6) keV γ ray, observed in coincidence with the 1026.2(0.3) keV transition, was assigned to the decay of the 2_2^+ state. The other suggested assignment of 0^+ for this state [22] requires an excitation of the two valence particles or the excitation of the core and is expected at a much higher energy. In ^{51}Ca, the 1943.4(5.7), 1466.3(1.6), and 843(2.7) keV transitions have not been observed earlier. A direct feeding (around 30%) to the 2^+ state in ^{52}Ca, found in the present work, was not observed in a two proton removal reaction [21]. Relatively large populations (normalized by the number of fragments) of 0.26(1) and 0.24(4) for the 2971.4(0.6) keV and 1426.1(3.2) keV γ rays for the decay of the known 3^- states in ^{50}Ca and ^{52}Ca, respectively, were observed in the present work. The equally strong feeding 0.17(6) of the state at a similar excitation energy ($\sim$4 MeV) in ^{51}Ca decaying by the 1466.3 keV transition suggests it to be an equivalent octupole state. Such a strong feeding of the octupole vibrational states has been observed earlier in other deep inelastic transfer studies [23].

In the following qualitative discussion, we utilize a simple shell model description with a doubly closed core of $^{48}_{20}$Ca$_{28}$ and the neutron single-particle energies in $^{49}_{20}$Ca to identify the expected dominant neutron configurations of the observed low-lying states in $^{50-52}$Ca. These are then used to experimentally obtain and study the evolution of the energy gaps between the $p_{1/2}$ and $f_{5/2}$ states as a function of isospin to address the question of a new shell gap at $N = 34$. Figure 4 shows restrictive level schemes of the Ca isotopes along with shell model calculations. The data for 1^+ states in ^{50,52}Ca and 2_3^+ state in ^{50}Ca are from Refs. [15,22].

As shown in Fig. 4 the ground state of ^{50}Ca corresponds to a pair of valence neutrons in the $p_{3/2}$ orbital coupled to $J^\pi = 0^+$ and a closed ^{48}Ca core. The first excited state (2^+) is identified with the breaking ($\simeq$1 MeV) of this pair. The next excitation is the promotion of a neutron to the $p_{1/2}$ orbital, which in analogy with the first excited state in ^{49}Ca, is expected to be 2 MeV above the 2_1^+ level. Only two states, namely, the 1^+ and 2^+ states, can be obtained from this $p_{3/2}p_{1/2}$ configuration. The requirement of antisymmetrization causes the spatial overlap of the wave function of two particles in the $p_{3/2}$ and $p_{1/2}$ orbitals in the 1^+ state to be inhibited relative to that in the 2^+ state [24]. This leads to the 2^+ level being more bound relative to the 1^+ state, as also predicted by the shell model calculation using the KB3GM interaction. The state at 4.9 MeV, also observed in β decay [22], is interpreted as 2^+ and a $p_{3/2}f_{5/2}$ excitation. A 1^+ assignment is unlikely because of the weak population of these (1^+) states in the present work. From the known energies of the low-lying states in ^{48}Ca the assignment of 3^-, 2_3^+, and 4^+ states are consistent with their identification as excitations of the core [2,22]. In ^{52}Ca, as the $p_{3/2}$ orbital is fully occupied in the ground state, the energy of the first 2^+ state is determined by the excitation of a neutron from the $p_{3/2}$ to $p_{1/2}$ orbital. The second excited state is analogous to the 1^+ state in ^{50}Ca [15]. The knowledge of the above states is now used to describe the structure of ^{51}Ca.

In ^{51}Ca, the three valence neutrons occupy the $p_{3/2}$ orbital, leading to a $3/2^-$ ground state; the excitation of one of these neutrons to the $p_{1/2}$ orbital (with the remaining two neutrons coupled to $J^\pi = 0^+$) leads to the first excited $1/2^-$ state. The next two excited states arise from coupling these two neutrons in the $p_{3/2}$ orbital to $J^\pi = 2^+$, giving rise to the $3/2^-$ and $5/2^-$ states. The $5/2^-$ state is lower in energy relative to $3/2^-$, as

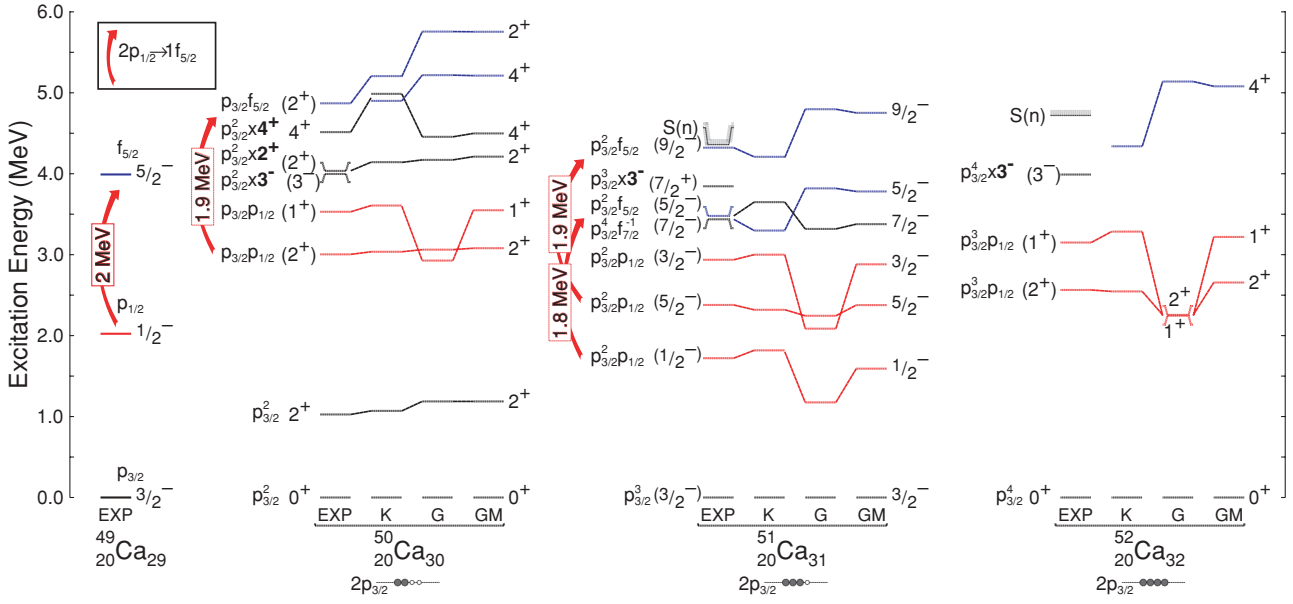

FIG. 4. (Color online) Restrictive level schemes of the Ca isotopes along with shell model calculations using KB3GM (K), GXPF1A (G), and a modified GXPF1A (GM) interaction (see text). The curved arrows connect states differing only with the promotion of a single neutron from $p_{1/2}$ to $f_{5/2}$ orbital with no change in the $(p_{3/2}^n, n = 0, 2)$ neutrons (see text).

is the case for the corresponding 2^+ and 1^+ states in ^{50}Ca. Higher lying states are formed either by excitation of one neutron to the $f_{5/2}$ state or by core excitations. A $5/2^-$ state can arise from the excitation of one neutron to the $f_{5/2}$ orbital with the remaining $p_{3/2}$ coupled to $J^\pi = 0^+$. Such a state is expected, from ^{49}Ca and ^{50}Ca, to be ~2 MeV above the $1/2^-$ state and, as seen from Fig. 4, is observed ~1.8 MeV above the $1/2^-$ state in ^{51}Ca. The breaking of the $p_{3/2}$ pair in the $p^2_{3/2}f_{5/2}$ configuration will result in a multiplet of states with the $9/2^-$ level expected to be the lowest. The position of this $9/2^-$ state, based on the energy difference between the $1/2^-_1$ and $5/2^-_1$ states of the $p^2_{3/2}p_{1/2}$ configuration is expected to lie ~0.7 MeV above the $5/2^-_2$ state. The observation of both the 843 keV γ ray corresponding to this expected difference and the 1943 keV transition to the $5/2^-_1$ level confirms this assignment. This excludes the states at 3.5 and 4.3 MeV to be associated with the excitation of the core. As discussed earlier, the state at 3.8 MeV is identified as $(p^3_{3/2} \times 3^-, 7/2^+)$ an octupole vibration; the other state at 3.4 MeV $(7/2^-)$ is identified with excitations of the ^{48}Ca core having a $p^4_{3/2}f^{-1}_{7/2}$ configuration.

The configurations of levels in terms of the valence neutrons and ^{48}Ca core excitations are discussed above and states having the relevant $p_{1/2}(p^n_{3/2}, J^\pi)$ and $f_{5/2}(p^n_{3/2}, J^\pi)$ configuration have been identified. The energy difference of ~1.9 MeV between these states represents the gap between the $p_{1/2}$ and $f_{5/2}$ neutron orbitals and is almost constant for all the isotopes as shown in Fig. 4. Shell model calculations predict a pure neutron configuration of greater than 75% for these states. This high purity of the wave function justifies the above approximation. In general, energy centroids obtained using the distribution of single-particle strength are to be used. Additional corrections to the derived gap can arise from the differences in the residual interaction of the $p_{1/2}$ or $f_{5/2}$ neutron with the $(p^n_{3/2}, J^\pi)$ spectator configuration. A simple extrapolation to ^{52}Ca would imply that the $E(4^+)$ state $(1f_{5/2}2p^3_{3/2})$ is at ~4.5 MeV. This is close to the neutron binding energy S_n of 4.7(7) MeV [25] and this state could be unbound. In ^{53}Ca, the $5/2^-$ state $(f_{5/2}(p^4_{3/2}, 0^+))$ is expected ~1.9 MeV above the $1/2^-$ ground state $(p_{1/2}(p^4_{3/2}, 0^+))$. The first excited state in ^{54}Ca is expected to be slightly higher than this value because of the additional stability of the ground state $(p^2_{1/2}, 0^+)(p^4_{3/2}, 0^+)$, similar to ^{52}Ca.

It can be seen from Fig. 4 that the energy differences between the $p_{1/2}$ and $f_{5/2}$ states obtained from the shell model calculations using the GXPF1A (KB3GM) interactions are 2.7(2.2) MeV in ^{50}Ca and 2.6(1.5) MeV and 2.6(1.9) MeV in ^{51}Ca. Thus the shell model calculations using the KB3GM interaction predict the corresponding energy differences ranging from 1.5 to 2.2 MeV and a relatively constant but large difference using the GXPF1A interaction. Both interactions are unable to reproduce the measured difference in energy between these states. Further, a comparison of the experimental levels with the predictions of the GXPF1A interaction in Fig. 4 shows a systematic lowering (by ~0.6 MeV) of states having a $\left|p_{3/2}p_{1/2}, 1^+\right\rangle$ parentage of the wave function (the 1^+ states in ^{50,52}Ca and $1/2^-, 3/2^-$ states in ^{51}Ca). Such a behavior can be traced back to a large

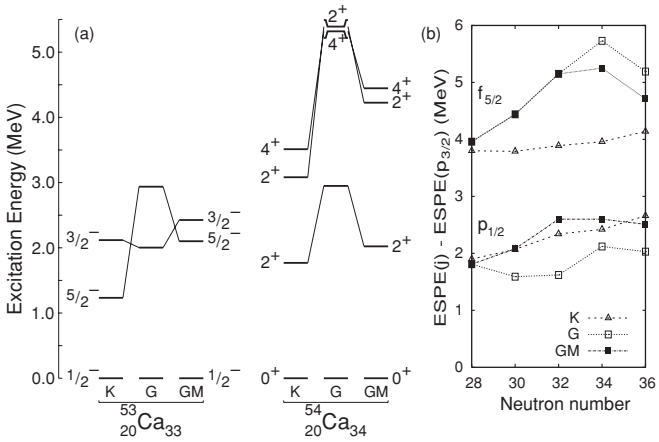

FIG. 5. (a) Shell model calculations using KB3GM (K), GXPF1A (G), and modified GXPF1A (GM) interactions for the lowest states in ^{53}Ca and ^{54}Ca (see text). (b) Effective single-particle energies (ESPE) of the neutron $p_{1/2}$ and $f_{5/2}$ orbits relative to the $p_{3/2}$ orbit in the Ca isotopes.

binding of the $\left\langle p_{3/2}p_{1/2}, 1^+ \left| V \right| p_{3/2}p_{1/2}, 1^+\right\rangle$ two-body matrix element $[V(1^+)]$ obtained for this interaction. It is possible that this matrix element is not well determined in the fitting procedure as its contribution to the natural parity states (in particular in nuclei with $Z > 20$) is expected to be small. In the GXPF1A interaction the matrix element $V(1^+)$ has a value of -0.159 MeV, which is relatively attractive and similar to that of the $V(2^+)$ matrix element with a value of -0.294 MeV. The corresponding values in the KB3GM interaction are $+0.552$ MeV and -0.288 MeV, respectively. The effect of this difference between the two interactions was studied from a modification of the GXPF1A interaction by setting $V(1^+) = +0.540$ MeV so as to reproduce the experimental $E(1^+)$ in ^{50}Ca. Calculations using this modified GXPF1A (GM) interaction are also shown in Fig. 4. As can be seen from the figure sizable shifts of the relevant energy levels are obtained resulting in a better description of the Ca isotopes.

Shown in Fig. 5(a) are shell model calculations for the lowest states in ^{53}Ca and ^{54}Ca using the same interactions used in Fig. 4. As can be seen in the figure the KB3GM (GXPF1A) interaction predicts an energy difference of 1.2(2.9) MeV between the $1/2^-$ and the $5/2^-$ states in ^{53}Ca. The corresponding calculations predict for the first 2^+ state in ^{54}Ca a value of 1.8(2.9) MeV. The results of shell model calculations using the modified GXPF1A interaction, which better reproduces the experimental level scheme in Fig. 4, demonstrate that the energy of the corresponding states in ^{53}Ca and ^{54}Ca are 1 MeV lower then those predicted using the GXPF1A interaction. Shown in Fig. 5(b) are the effective single-particle energies of the neutron $2p_{1/2}$ and $1f_{5/2}$ orbits relative to the $2p_{3/2}$ orbit in the Ca isotopes. The KB3GM (GXPF1A) interaction predicts for the $N = 34$ gap a value of 1.5(3.6) MeV. It can be seen that the modification of the $\left\langle p_{3/2}p_{1/2}, 1^+ \left| V \right| p_{3/2}p_{1/2}, 1^+\right\rangle$ matrix element in the GXPF1A interaction reduces the predicted gap at $N = 34$ to 2.6 MeV. The above modification does not account for the predicted higher excitation energy of the levels involving the $f_{5/2}$ orbit and, when considered,

would lead to a further reduction in this gap. It should be noted that the modification described above of the GXPF1A interaction has an impact only on the predicted $N = 34$ shell gap in Ca. Calculations using this modification were seen to have a weak influence on the calculated yrast structures in neighboring isotopes of Ti or Cr, thus maintaining the excellent agreement of the calculations with the experimental data. It is because of the above described reasons that the predicted energy spacing between the $p_{1/2}$ and $f_{5/2}$ orbitals using the GXPF1A interaction is large compared to that experimentally obtained. Thus the lack of evolution of the gap for increasing isospin and the inconsistency of the prediction [5] with the experimental data appear to contradict the existence of a new "magic number" at $N = 34$.

In summary, this work presents new limits of experimental sensitivity to access a wide variety of states with different configurations necessary to study structural changes far from stability. A shell model interpretation of the measured levels of the neutron-rich isotopes of Ca shows that the energy spacing between the $2p_{1/2}$ and $1f_{5/2}$ neutron orbitals is almost constant going from $^{49-52}$Ca and, when extrapolated to ^{53,54}Ca, shows that $N = 34$ may not appear to be a new magic number. Measurements of the lowest $f_{5/2}$ state in ^{53}Ca and/or the first 2^+ state in ^{54}Ca would provide additional information for the understanding of a $N = 34$ shell closure and help to improve modern realistic residual interactions.

The authors are thankful to the GANIL team for their flawless operation of the facility. They would like to thank B. Lecornu, C. Marry, J. Ropert, G. Voltolini, Ch. Spitaels, and G. Fremont for their dedicated and untiring efforts in the operation of the detection systems and M. Rousseau and R. Chapman for their assistance in taking the data. They also thank the Strasbourg-Madrid shell model collaboration for providing the shell model interactions and many stimulating discussions and K. Heyde and P. Van Isacker for a critical reading of the manuscript. The INTAG under EURONS is thanked for support.

[1] H. Nishioka, Z. Phys. D **19**, 19 (1991).
[2] R. Broda, J. Phys. G **32**, R151 (2006).
[3] E. Caurier *et al*., Rev. Mod. Phys. **77**, 427 (2005); A. Poves *et al*., Nucl. Phys. **A694**, 157 (2001).
[4] B. A. Brown and W. A. Richter, Phys. Rev. C **74**, 034315 (2006).
[5] M. Honma, T. Otsuka, B. A. Brown, and T. Mizusaki, Phys. Rev. C **69**, 034335 (2004); M. Honma *et al*., Eur. Phys. J. A **25**, Suppl. 1, 499 (2005).
[6] T. Otsuka, T. Suzuki, R. Fujimoto, H. Grawe, and Y. Akaishi, Phys. Rev. Lett. **95**, 232502 (2005).
[7] A. Bohr and B. R. Mottelson, *Nuclear Structure* (Benjamin, Reading, MA, 1975), Vol. I.
[8] A. Huck *et al*., Phys. Rev. C **31**, 2226 (1985).
[9] J. I. Prisciandaro *et al*., Phys. Lett. **B510**, 17 (2001).
[10] R. V. F. Janssens *et al*., Phys. Lett. **B546**, 55 (2002).
[11] M. Beiner, R. J. Lombard, and D. Mas, Nucl. Phys. **A249**, 1 (1975).
[12] D. C. Dinca *et al*., Phys. Rev. C **71**, 041302(R) (2005).
[13] B. Fornal *et al*., Phys. Rev. C **72**, 044315 (2005).
[14] N. Marginean *et al*., Phys. Lett. **B633**, 696 (2006).
[15] F. Perrot *et al*., Phys. Rev. C **74**, 014313 (2006).
[16] E. Caurier *et al*. (to be published); F. Nowacki (private communication, 2006).
[17] R. Broda *et al*., Phys. Lett. **B251**, 245 (1990).
[18] B. Fornal *et al*., Phys. Rev. C **70**, 064304 (2004).
[19] H. Savajols *et al*., Nucl. Phys. **A654**, 1027c (1999).
[20] J. Simpson *et al*., Acta Phys. Hung. New Ser.: Heavy Ion Phys. **11**, 159 (2000).
[21] A. Gade *et al*., Phys. Rev. C **74**, 021302(R) (2006).
[22] P. Baumann *et al*., Phys. Rev. C **58**, 1970 (1998).
[23] M. Rejmund *et al*., Eur. Phys. J. A **8**, 161 (2000).
[24] R. F. Casten, *Nuclear Structure from a Simple Perspective* (Oxford Univ. Press, London, 2001), p. 103.
[25] G. Audi *et al*., Nucl. Phys. **A729**, 337 (2003).